

pubs.acs.org/JACS Communication

Chain-End Functionalized Polymers for the Controlled Synthesis of Sub-2 nm Particles

Peng-Cheng Chen, Yuan Liu, Jingshan S. Du, Brian Meckes, Vinayak P. Dravid, and Chad A. Mirkin*



Cite This: J. Am. Chem. Soc. 2020, 142, 7350-7355



ACCESS

Metrics & More



Supporting Information

ABSTRACT: A novel method for synthesizing arrays of uniform sub-2 nm particles on substrates is described. Such particles are made by (i) using dip-pen nanolithography to prepare nanoreactors consisting of metal-coordinated polymers; (ii) designing polymers with only one metal atom attached to each polymer chain; (iii) systematically controlling nanoreactor volume down to the yoctoliter scale; and (iv) transforming each nanoreactor into a metal nanoparticle through thermal annealing. Polymer design in this study is crucial, since it allows one to tightly control nanoparticle size by tuning the volume of the polymer reactors, which correlates with the number of polymer chains and, therefore, metal atoms. Mixtures of different metal-functionalized polymers were used to synthesize ultrasmall alloy particles. The technique and results described herein point toward a way of using these novel polymers to systematically explore the properties and uses of this important class of nanomaterials in many fields.

Tanoparticles that have fewer than 300 atoms and diameters less than 2 nm, commonly referred to as nanoclusters, have attracted extensive interest due to their properties that differ from single atoms and larger colloidal nanoparticles.^{1–4} When nanoparticles approach the nanocluster regime, the particles exhibit discrete molecular orbitals, in contrast with the energy bands characteristic of larger metal nanoparticles.⁴⁻⁷ In addition, the high surface-area-to-volume ratio of nanoclusters makes their geometric structures highly dependent on their environment such as solvents and supports.^{4,8} These electronic and geometric structural characteristics give nanoclusters interesting catalytic, 9-16 optical, 17,18 and magnetic properties. 19,20 Currently, many methods have been established to synthesize ultrasmall nanoparticles. 21-33 For example, by controlling the nucleation and growth process, bulk solution-based synthesis can be used to synthesize nanoclusters with a precise number of atoms. 11-13,21-23 Alternatively, nanoclusters can be accessed utilizing nanoreactor-mediated synthesis, 24-30 where the nanoreactor (e.g., dendrimers, star-shaped polymers, and molecular cages) restricts the growth of the particles by limiting the amount of precursor present.

Recently, we developed a technique, termed scanning probe block copolymer lithography, that combines nanoreactor-mediated synthesis and scanning probe lithography to realize site-specific synthesis of 2.5–60 nm nanoparticles, some with as many as seven elements (Au, Ag, Cu, Pd, Ni, Co, and Sn).^{34–44} This method typically relies on an atomic force microscope (AFM) tip to print attoliter-scale volumes of metal-coordinated poly(ethylene oxide)-*b*-poly(2-vinylpyridine) (PEO-*b*-P2VP) nanoreactors onto a substrate in a site-specific manner. The metal precursors are then thermally converted under Ar or H₂ into a nanoparticle within each nanoreactor.

Thus far, no methods have been developed to make sub-2 nm particles in a site-isolated manner, yet the realization of

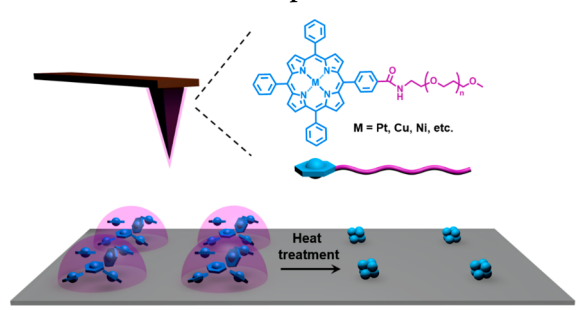
such capabilities could open avenues to a wide variety of functional devices that take advantage of size- and compositionally dependent properties uniquely associated with such particles. 45,46 Unfortunately, attempts to make sub-2 nm particles with PEO-b-P2VP nanoreactors by scaling down the metal loading, or the volume of the reactors led to very nonuniform distributions of particles. When the nanoreactors approach very small volumes, the metal precursor content from reactor to reactor becomes highly variable due to the nonuniform dispersion of the metal precursor in the PEO-b-P2VP ink. Consequently, some nanoreactors produce particles larger than 2 nm particles, and some reactors are empty. In an attempt to circumvent this problem, we designed and synthesized a novel porphyrin-capped PEO that has a fixed stoichiometry between metal atoms and polymers and can be deliberately loaded with different metals via the porphyrin functionality (Scheme 1). We hypothesized that, by fixing the number of metal ions per polymer chain, more uniform nanoreactors could be generated, which in turn would yield ultrasmall nanoparticles with tighter control over size. With this approach and a Pt²⁺-loaded polymer as the ink, nanoreactors with deliberately controlled volumes down to the yoctoliter scale were printed using dip-pen nanolithography (DPN); these nanoreactors were thermally converted into Pt nanoparticles with controlled sizes ranging from 1 to 5 nm. Moreover, we used the technique to synthesize binary and ternary ultrasmall particles consisting of combinations of Cu,

Received: February 25, 2020 Published: April 13, 2020





Scheme 1. Scheme for the Polymer Nanoreactor-mediated Synthesis of Ultrasmall Nanoparticles^a



"Metalloporphyrin-terminated poly(ethylene oxide) is used as an ink and deposited onto a substrate at desired locations via DPN. The substrate is thermally annealed to decompose the polymers to yield a single nanoparticle in every polymer nanoreactor.

Ni, and Pt by using a mixture of metalloporphyrin-terminated polymers as the ink.

The targeted polymers were synthesized by coupling 5,10,15-triphenyl-20-(4-carboxyphenyl) porphyrin (with or without metal, depending on metal choice) with methoxy-PEO5k amine ($M_n = 5000$) via a hexafluorophosphate azabenzotriazole tetramethyl uronium (HATU)-mediated amidation. The 1:1 reaction between the two reactants leads to the desired porphyrin-capped polymer (metalated or metalfree tetraphenylporphyrin-PEO, denoted as MTPP-PEO5k and TPP-PEO5k, respectively). In the case of the metal-free polymer (TPP-PEO5k), it can be postmetalated with Cu²⁺, Ni²⁺, Co²⁺, or Zn²⁺ by mixing it with metal acetate salts at 80 °C for 24 h (see Supporting Information). For metal ions that require harsher loading conditions such as Pt²⁺ (~190 °C for 24 h), we coordinated the metals with the porphyrin molecules first and then coupled the metalloporphyrins to the end of the PEO chains.

Matrix-assisted laser desorption ionization time-of-flight mass spectrometry (MALDI-TOF MS) characterization was performed on PEO5k and TPP-PEO5k, respectively, to characterize the capping of a porphyrin to the PEO. As shown in Figures 1A and S1, the starting material (PEO5k) has a number-average molecular weight (M_n) of 5265 and a dispersity (D) of 1.005. After the coupling reaction, the M_n of the polymers increases from 5265 to 5906, while the D (1.004) remains unaffected. The increase in M_n by 641 is consistent with the expected increase in M_n (640.7) that would result from the addition of a single porphyrin to the PEO. To explore whether we could use the porphyrin-capped polymer for synthesizing single-metal atom-coordinated polymers, we investigated the metal loading process by UV-vis spectroscopy. The porphyrin has 18 conjugated and delocalized π electrons that can lead to two types of light absorption bands, that is, B-band and Q-band. Figures 1B and S2 show the UV-vis spectra of TPP-PEO5k and different metal-loaded TPP-PEO5k. TPP-PEO5k exhibits a strong absorption peak at 418 nm (B-band) and four characteristic weak absorption bands between 500 and 750 nm (Q-band), which is consistent with the UV-vis spectrum of tetraphenylporphyrin (TPP, Figure S3). The UV-vis spectrum of the polymer changes after metal loading. When one compares the UV-vis spectra of metal-loaded TPP-PEO5k and the spectra of corresponding metalloporphyrins (Figures 1B, S2, and S3), the shape and position of both the Q-band and B-band peaks are consistent,

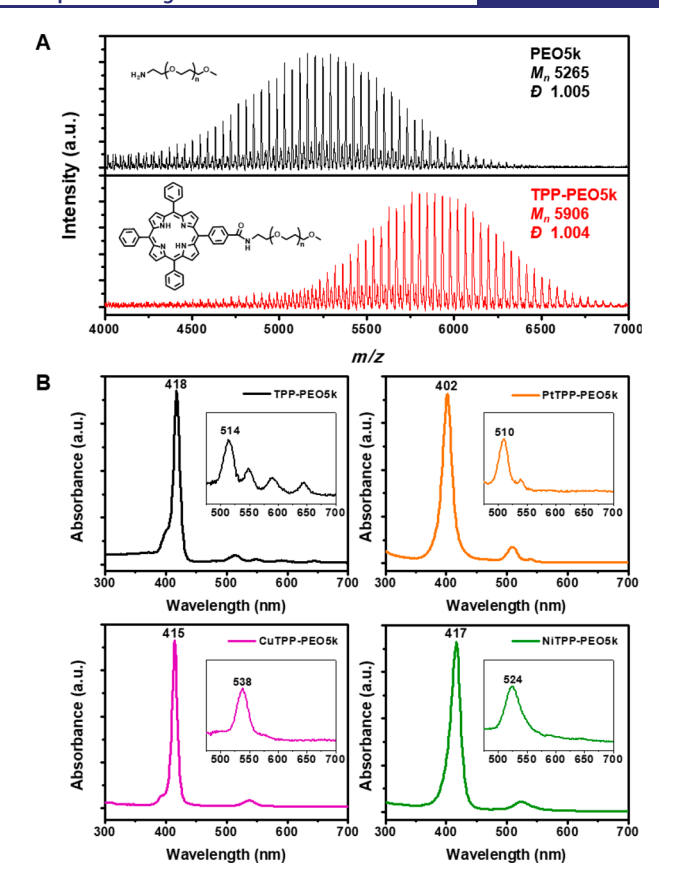


Figure 1. Characterization of the chain-end functionalized polymers. (A) MALDI-TOF MS spectra of PEO5k and TPP-PEO5k. (B) UV–vis absorption spectra of TPP-PEO5k, PtTPP-PEO5k, CuTPP-PEO5k, and NiTPP-PEO5k in dichloromethane. (inset) Enlarged absorption spectra of the range of 475–700 nm.

confirming that virtually every porphyrin in the chain-end functionalized PEO is coordinated to a metal.

Following metal complexation with the porphyrin-capped polymers, we printed the polymers on a hydrophobic TEM grid in the form of dome-shaped reactors via DPN. Experimentally, polymer dots with diameters ranging from less than 20 to 330 nm were obtained by modulating the DPN probe-substrate contact time from 1 to 50 ms (Figures S4 and S5). AFM topographical characterization was used to determine the volume of each polymer nanoreactor. Since each PEO chain contains only one metal atom, the total number of metal atoms in a polymer dot can be estimated from the volume of the polymer dots (Figures S4C and S6, assuming that the polymer dots have a similar density to PEO, 1.2 g/ mL). For PtTPP-PEO5k dots with diameters of ~35 nm, the measured volume is ~2 zL, which corresponds to 295 Pt atoms. When the diameter of PtTPP-PEO5k dots were further decreased to less than 20 nm, the volume is less than 400 yL, and the total number of Pt atoms is less than 50. Therefore, by printing polymer dots smaller than 35 nm in diameter, we can create nanoreactors containing fewer than 300 metal atoms.

Next, we annealed the PtTPP-PEOSk dots in a stepwise fashion at elevated temperatures (160–600 °C) and then characterized the products using aberration-corrected high-angle annular dark-field scanning transmission electron microscopy (HAADF-STEM). Remarkably, single nanoparticles are found in place of each polymer nanoreactor after annealing (Figures 2, S7, and S8). Energy-dispersive X-ray

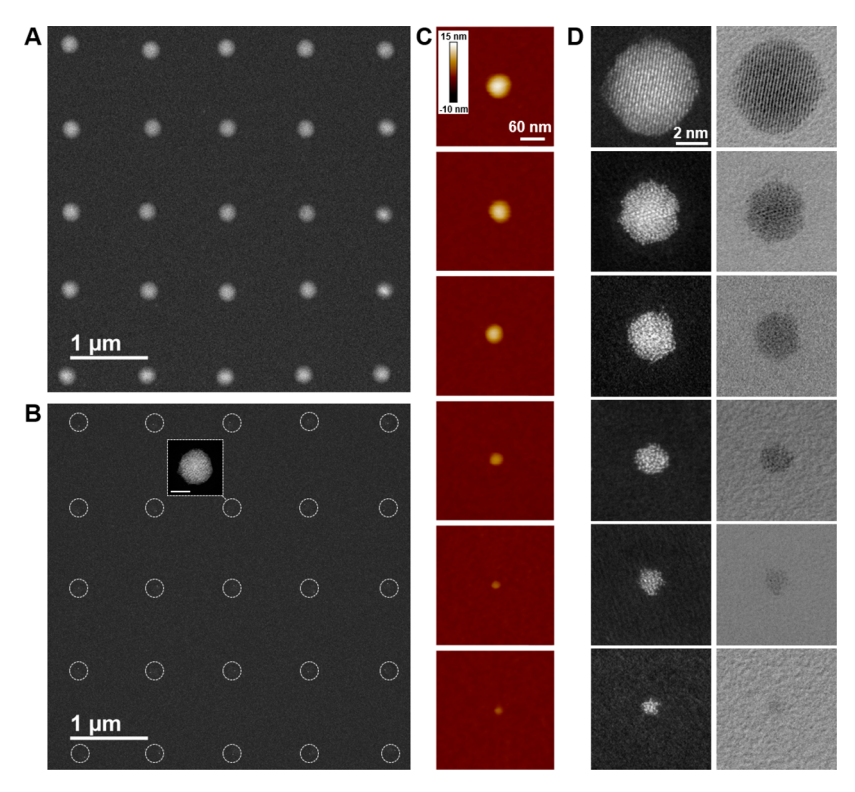


Figure 2. Polymer nanoreactor-mediated synthesis of Pt nanoparticles. (A) HAADF-STEM image of a representative 5×5 array of polymer nanoreactors. (B) HAADF-STEM image of nanoparticles obtained after thermally annealing the polymer nanoreactors. Dotted circles indicate the location of the nanoreactors, prior to annealing. Scale bar in inset: 3 nm. (C) AFM topographical images of polymer nanoreactors with diameters ranging from 65 to less than 20 nm. (D) HAADF-STEM and BF-STEM images of nanoparticles obtained from polymer nanoreactors of diameters corresponding to those shown in (C). The nanoparticle diameters range from 5 to \sim 1 nm.

spectroscopy (EDS) and X-ray photoelectron spectroscopy (XPS) analysis confirm that the observed nanoparticles are composed of Pt (Figures S9–S12). To validate the hypothesis that molecularly pure inks can improve the control over particle size, we explored the correlation between nanoparticle size and polymer nanoreactor size. From these studies, we found that the sizes of the polymer dots and nanoparticles are positively correlated. Specifically, when the diameter of the polymer dots decreased from 65 to 25 nm (Figure 2C), the average diameter of the nanoparticles decreased accordingly from 5.2 to 1.3 nm with a standard deviation less than 0.4 nm (Figures 2D and 3). Importantly, the size of the resulting nanoparticles is within the theoretical size range (Figure S13).

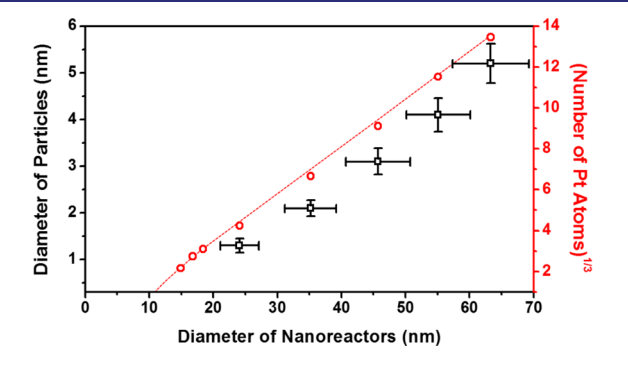


Figure 3. Comparison between the size of the deposited nanoreactors, the size of the resulting nanoparticles, and the theoretical number of metal atoms in each nanoreactor. The theoretical number of metal atoms in each nanoreactor is estimated based on nanoreactor volume (Figures S5 and S6). Dashed line is a guide.

For instance, an ~ 35 nm polymer nanoreactor that contains ~ 295 Pt atoms should yield either a Pt sphere with a diameter of 2.0 nm or a Pt hemisphere with a diameter of ~ 2.5 nm (Figures 3 and S13), which agrees well with the measured size of our nanoparticles $(2.1 \pm 0.2 \text{ nm})$. For polymer nanoreactors less than 20 nm, which contain fewer than 50 Pt atoms, it becomes challenging to accurately measure the size of the resulting ultrasmall nanoparticles, because the nanoparticles are unstable under an electron beam, which results in images with irregular particle shapes (Figure 4). In addition to structural instability, single Pt atoms are continuously dislodged from the Pt nanoparticles when the particles are irradiated by an electron beam (Figure S14). Since the overall

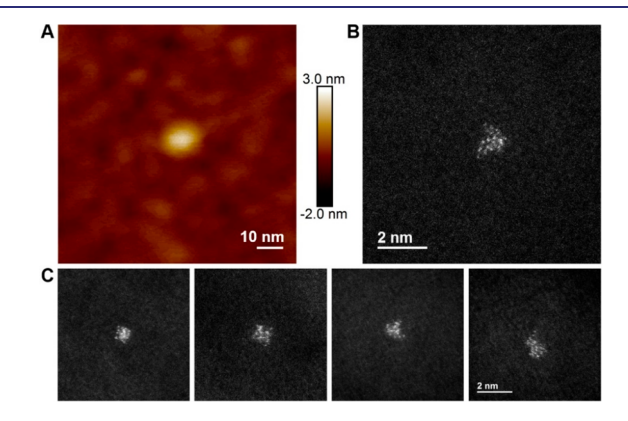


Figure 4. (A) AFM topographical image of a polymer nanoreactor with a diameter less than 20 nm. (B, C) HAADF-STEM images of Pt nanoparticles synthesized from ultrasmall nanoreactors (<20 nm).

number of Pt atoms is less than 50 in this scenario, the dislodged atoms become non-negligible when evaluating the particle size.

One attractive feature of nanoreactor-mediated synthesis is the ability to incorporate diverse metal precursors into a reactor and then convert such precursors into a single nanoparticle through the aggregation of all metal species in the reactor. ^{24,27,41} To validate the applicability of our new polymer system for generating polyelemental nanoparticles, we added equal amounts of CuTPP-PEO5k (or NiTPP-PEO5k) to PtTPP-PEO5k and stirred for 24 h. Nanoreactors were printed via DPN using the mixtures as inks and converted into nanoparticles via thermal treatment (Figure 5A). As shown in

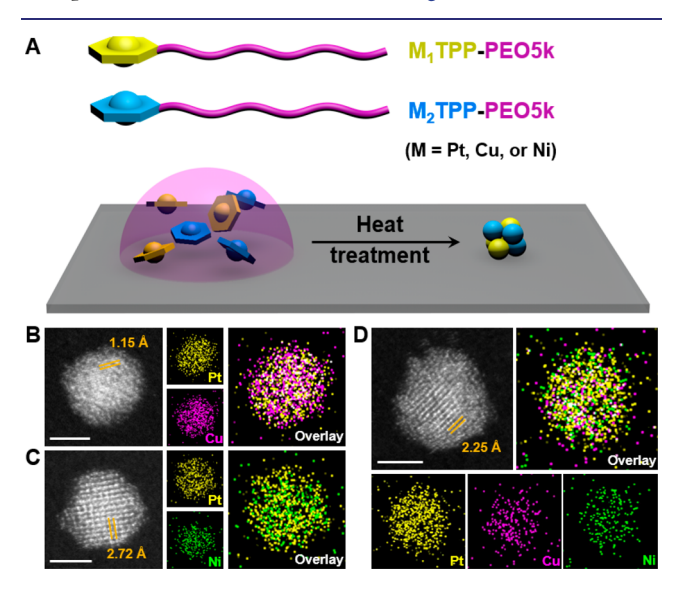


Figure 5. Polymer-mediated synthesis of ultrasmall polyelemental nanoparticles. (A) Scheme depicting the synthesis of polyelemental nanoparticles by blending different metal-coordinated polymers. (B–D) HAADF-STEM images and EDS elemental maps of PtCu (Pt $_{0.41}$ Cu $_{0.59}$), PtNi (Pt $_{0.59}$ Ni $_{0.41}$), and PtCuNi (Pt $_{0.62}$ Cu $_{0.19}$ Ni $_{0.19}$) nanoparticles synthesized from mixtures of metalloporphyrin-terminated polymers. Scale bars: 2 nm.

Figures 5B,C and S15, PtCu and PtNi alloy nanoparticles were successfully synthesized from nanoreactors containing blended metalloporphyrin-terminated polymers. The even contrast of the HAADF-STEM images of nanoparticles indicates alloying within each binary system, which is further evidenced by the overlap of the EDS elemental maps. The observed lattice spacings are 1.15 and 2.72 Å, which match the (311) plane of a face-centered cubic PtCu alloy and the (100) plane of a facecentered tetragonal PtNi alloy, respectively. In addition to bimetallic particles, PtCuNi trimetallic nanoparticles (Figures 5D and S15) can be synthesized by blending PtTPP-PEO5k, CuTPP-PEO5k, and NiTPP-PEO5k (2:1:1, molar ratio). Taken together, this study of polyelemental nanoparticles demonstrates that nanoreactors consisting of mixed metalloporphyrin-terminated polymers can be used to access ultrasmall polyelemental nanoparticles.

In summary, we reported the site-specific synthesis of ultrasmall nanoparticles using nanoreactors made by single-metal atom-functionalized polymers. The design of metal-loporphyrin-terminated polymers fixes the stoichiometry between metal atoms and polymers. Consequently, sub-2 nm nanoparticles can be synthesized in polymer nanoreactors in a

size-controlled and site-specific manner. In addition to corroborating the general applicability of using polymer nanoreactors to synthesize nanoparticles, this study also illustrates that the careful design of polymers provides an important way to control nanoparticle composition and size, expanding the library of possibilities available through nanoreactor-mediated synthesis. Given the vast polymer design space, this research will open a new route to accessing novel nanostructures in a site-specific manner. Such nanostructures may have important applications in catalysis, magnetics, optics, and many other fields. 44–46

ASSOCIATED CONTENT

Supporting Information

The Supporting Information is available free of charge at https://pubs.acs.org/doi/10.1021/jacs.0c02244.

Experimental section, UV-vis spectra of metalloporphyrins, AFM images of polymer nanoreactors, TGA analysis of polymers, HAADF-STEM images and EDS analysis of nanoparticles, XPS analysis of polymer residues and nanoparticles (PDF)

AUTHOR INFORMATION

Corresponding Author

Chad A. Mirkin — Department of Materials Science and Engineering, International Institute for Nanotechnology, and Department of Chemistry, Northwestern University, Evanston, Illinois 60208, United States; Occid.org/0000-0002-6634-7627; Email: chadnano@northwestern.edu

Authors

Peng-Cheng Chen — Department of Materials Science and Engineering and International Institute for Nanotechnology, Northwestern University, Evanston, Illinois 60208, United States; ○ orcid.org/0000-0002-0411-9549

Yuan Liu — International Institute for Nanotechnology and Department of Chemistry, Northwestern University, Evanston, Illinois 60208, United States

Jingshan S. Du — Department of Materials Science and Engineering and International Institute for Nanotechnology, Northwestern University, Evanston, Illinois 60208, United States; © orcid.org/0000-0002-4932-6699

Brian Meckes — International Institute for Nanotechnology and Department of Chemistry, Northwestern University, Evanston, Illinois 60208, United States; orcid.org/0000-0002-8389-4622

Vinayak P. Dravid — Department of Materials Science and Engineering and International Institute for Nanotechnology, Northwestern University, Evanston, Illinois 60208, United States; © orcid.org/0000-0002-6007-3063

Complete contact information is available at: https://pubs.acs.org/10.1021/jacs.0c02244

Author Contributions

These authors contributed equally to this work.

Notes

The authors declare the following competing financial interest(s): A provisional patent application has been filed on this work. C.A.M. has financial interests in TERA-print, LLC which could potentially benefit from the outcomes of this research.

■ ACKNOWLEDGMENTS

This material is based upon work supported by the Sherman Fairchild Foundation, Inc., the National Science Foundation (NSF) Award Nos. CHE-1709888 and IIP-1621773, the U.S. Army Award No. W911NF-15-1-0151, and the Air Force Office of Scientific Research Award No. FA9550-17-1-0348. B.M. acknowledges support from the Eden and Steven Romick Post-Doctoral Fellowship through the American Committee for the Weizmann Institute of Science. This work made use of the EPIC and the Keck-II facilities of Northwestern University's NUANCE Center, which has received support from the Soft and Hybrid Nanotechnology Experimental (SHyNE) Resource (NSF ECCS-1542205); the MRSEC program (NSF DMR-1720139) at the Materials Research Center; the International Institute for Nanotechnology (IIN); the Keck Foundation; and the State of Illinois, through the IIN.

REFERENCES

- (1) Li, G.; Jin, R. C. Atomically Precise Gold Nanoclusters as New Model Catalysts. *Acc. Chem. Res.* **2013**, *46*, 1749.
- (2) Hossain, S.; Niihori, Y.; Nair, L. V.; Kumar, B.; Kurashige, W.; Negishi, Y. Alloy Clusters: Precise Synthesis and Mixing Effects. *Acc. Chem. Res.* **2018**, *51*, 3114.
- (3) Jin, R. C.; Zeng, C. J.; Zhou, M.; Chen, Y. X. Atomically Precise Colloidal Metal Nanoclusters and Nanoparticles: Fundamentals and Opportunities. *Chem. Rev.* **2016**, *116*, 10346.
- (4) Liu, L. C.; Corma, A. Metal Catalysts for Heterogeneous Catalysis: From Single Atoms to Nanoclusters and Nanoparticles. *Chem. Rev.* **2018**, *118*, 4981.
- (5) Kaden, W. E.; Wu, T. P.; Kunkel, W. A.; Anderson, S. L. Electronic Structure Controls Reactivity of Size-Selected Pd Clusters Adsorbed on TiO2 Surfaces. *Science* **2009**, *326*, 826.
- (6) Liu, Y. M.; Tsunoyama, H.; Akita, T.; Xie, S. H.; Tsukuda, T. Aerobic Oxidation of Cyclohexane Catalyzed by Size-Controlled Au Clusters on Hydroxyapatite: Size Effect in the Sub-2 nm Regime. ACS Catal. 2011, 1, 2.
- (7) Zhu, M.; Aikens, C. M.; Hollander, F. J.; Schatz, G. C.; Jin, R. Correlating the crystal structure of A thiol-protected Au-25 cluster and optical properties. *J. Am. Chem. Soc.* **2008**, *130*, 5883.
- (8) Moliner, M.; Gabay, J. E.; Kliewer, C. E.; Carr, R. T.; Guzman, J.; Casty, G. L.; Serna, P.; Corma, A. Reversible Transformation of Pt Nanoparticles into Single Atoms inside High-Silica Chabazite Zeolite. *J. Am. Chem. Soc.* **2016**, *138*, 15743.
- (9) Yan, H.; Cheng, H.; Yi, H.; Lin, Y.; Yao, T.; Wang, C. L.; Li, J. J.; Wei, S. Q.; Lu, J. L. Single-Atom Pd-1/Graphene Catalyst Achieved by Atomic Layer Deposition: Remarkable Performance in Selective Hydrogenation of 1,3-Butadiene. J. Am. Chem. Soc. 2015, 137, 10484.
- (10) Tyo, E. C.; Vajda, S. Catalysis by clusters with precise numbers of atoms. *Nat. Nanotechnol.* **2015**, *10*, 577.
- (11) Zhu, Y.; Qian, H. F.; Drake, B. A.; Jin, R. C. Atomically Precise Au-25(SR)(18) Nanoparticles as Catalysts for the Selective Hydrogenation of alpha, beta-Unsaturated Ketones and Aldehydes. *Angew. Chem., Int. Ed.* **2010**, 49, 1295.
- (12) Zhang, H. J.; Lu, L. L.; Kawashima, K.; Okumura, M.; Haruta, M.; Toshima, N. Synthesis and Catalytic Activity of Crown Jewel-Structured (IrPd)/Au Trimetallic Nanoclusters. *Adv. Mater.* **2015**, 27, 1383.
- (13) Wang, T. Y.; Liang, J. S.; Zhao, Z. L.; Li, S. Z.; Lu, G.; Xia, Z. C.; Wang, C.; Luo, J. H.; Han, J. T.; Ma, C.; Huang, Y. H.; Li, Q. Sub-6 nm Fully Ordered L1(0)-Pt-Ni-Co Nanoparticles Enhance Oxygen Reduction via Co Doping Induced Ferromagnetism Enhancement and Optimized Surface Strain. *Adv. Energy Mater.* **2019**, *9*, 1803771.
- (14) Herzing, A. A.; Kiely, C. J.; Carley, A. F.; Landon, P.; Hutchings, G. J. Identification of active gold nanoclusters on iron oxide supports for CO oxidation. *Science* **2008**, *321*, 1331.

- (15) Lei, Y.; Mehmood, F.; Lee, S.; Greeley, J.; Lee, B.; Seifert, S.; Winans, R. E.; Elam, J. W.; Meyer, R. J.; Redfern, P. C.; Teschner, D.; Schlogl, R.; Pellin, M. J.; Curtiss, L. A.; Vajda, S. Increased Silver Activity for Direct Propylene Epoxidation via Subnanometer Size Effects. *Science* **2010**, 328, 224.
- (16) Yang, M.; Li, S.; Wang, Y.; Herron, J. A.; Xu, Y.; Allard, L. F.; Lee, S.; Huang, J.; Mavrikakis, M.; Flytzani-Stephanopoulos, M. Catalytically active Au-O(OH)(x)-species stabilized by alkali ions on zeolites and mesoporous oxides. *Science* **2014**, *346*, 1498.
- (17) Kang, X.; Zhu, M. Z. Tailoring the photoluminescence of atomically precise nanoclusters. *Chem. Soc. Rev.* **2019**, *48*, 2422.
- (18) Hu, X. Q.; Zheng, Y. K.; Zhou, J. Y.; Fang, D. J.; Jiang, H.; Wang, X. M. Silver-Assisted Thiolate Ligand Exchange Induced Photoluminescent Boost of Gold Nanoclusters for Selective Imaging of Intracellular Glutathione. *Chem. Mater.* **2018**, *30*, 1947.
- (19) Jamet, M.; Wernsdorfer, W.; Thirion, C.; Mailly, D.; Dupuis, V.; Melinon, P.; Perez, A. Magnetic anisotropy of a single cobalt nanocluster. *Phys. Rev. Lett.* **2001**, *86*, 4676.
- (20) Sljivancanin, Z.; Pasquarello, A. Supported Fe nanoclusters: Evolution of magnetic properties with cluster size. *Phys. Rev. Lett.* **2003**, *90*, 247202.
- (21) Zhu, M.; Lanni, E.; Garg, N.; Bier, M. E.; Jin, R. Kinetically controlled, high-yield synthesis of Au-25 clusters. *J. Am. Chem. Soc.* **2008**, *130*, 1138.
- (22) Heaven, M. W.; Dass, A.; White, P. S.; Holt, K. M.; Murray, R. W. Crystal structure of the gold nanoparticle N(C8H17)(4) Au-25(SCH2CH2Ph)(18). J. Am. Chem. Soc. 2008, 130, 3754.
- (23) Wong, A.; Liu, Q.; Griffin, S.; Nicholls, A.; Regalbuto, J. R. Synthesis of ultrasmall, homogeneously alloyed, bimetallic nanoparticles on silica supports. *Science* **2017**, *358*, 1427.
- (24) Scott, R. W. J.; Datye, A. K.; Crooks, R. M. Bimetallic palladium-platinum dendrimer-encapsulated catalysts. *J. Am. Chem. Soc.* **2003**, *125*, 3708.
- (25) Iyyamperumal, R.; Zhang, L.; Henkelman, G.; Crooks, R. M. Efficient Electrocatalytic Oxidation of Formic Acid Using Au@Pt Dendrimer-Encapsulated Nanoparticles. *J. Am. Chem. Soc.* **2013**, *135*, 5521.
- (26) Imaoka, T.; Akanuma, Y.; Haruta, N.; Tsuchiya, S.; Ishihara, K.; Okayasu, T.; Chun, W. J.; Takahashi, M.; Yamamoto, K. Platinum clusters with precise numbers of atoms for preparative-scale catalysis. *Nat. Commun.* **2017**, *8*, 688.
- (27) Tsukamoto, T.; Kambe, T.; Nakao, A.; Imaoka, T.; Yamamoto, K. Atom-hybridization for synthesis of polymetallic clusters. *Nat. Commun.* **2018**, *9*, 3873.
- (28) Pang, X. C.; Zhao, L.; Han, W.; Xin, X. K.; Lin, Z. Q. A general and robust strategy for the synthesis of nearly monodisperse colloidal nanocrystals. *Nat. Nanotechnol.* **2013**, *8*, 426.
- (29) Chen, Y. H.; Yang, D.; Yoon, Y. J.; Pang, X. C.; Wang, Z. W.; Jung, J. H.; He, Y. J.; Harn, Y. W.; He, M.; Zhang, S. G.; Zhang, G. Z.; Lin, Z. Q. Hairy Uniform Permanently Ligated Hollow Nanoparticles with Precise Dimension Control and Tunable Optical Properties. *J. Am. Chem. Soc.* 2017, 139, 12956.
- (30) McCaffrey, R.; Long, H.; Jin, Y. H.; Sanders, A.; Park, W.; Zhang, W. Template Synthesis of Gold Nanoparticles with an Organic Molecular Cage. *J. Am. Chem. Soc.* **2014**, *136*, 1782.
- (31) Gologan, B.; Green, J. R.; Alvarez, J.; Laskin, J.; Graham Cooks, R. Ion/surface reactions and ion soft-landing. *Phys. Chem. Chem. Phys.* **2005**, *7*, 1490.
- (32) Johnson, G. E.; Wang, C.; Priest, T.; Laskin, J. Monodisperse Au-11 Clusters Prepared by Soft Landing of Mass Selected Ions. *Anal. Chem.* **2011**, *83*, 8069.
- (33) Johnson, G. E.; Hu, Q. C.; Laskin, J.; Cooks, R. G.; Yeung, E. S. Soft Landing of Complex Molecules on Surfaces. *Annu. Rev. Anal. Chem.* **2011**, *4*, 83 DOI: 10.1146/annurev-anchem-061010-114028.
- (34) Javey, A.; Dai, H. J. Regular arrays of 2 nm metal nanoparticles for deterministic synthesis of nanomaterials. *J. Am. Chem. Soc.* **2005**, 127, 11942.

- (35) Jibril, L.; Chen, P. C.; Hu, J. T.; Odom, T. W.; Mirkin, C. A. Massively Parallel Nanoparticle Synthesis in Anisotropic Nanoreactors. *ACS Nano* **2019**, *13*, 12408.
- (36) Cheng, W. L.; Park, N. Y.; Walter, M. T.; Hartman, M. R.; Luo, D. Nanopatterning self-assembled nanoparticle superlattices by moulding microdroplets. *Nat. Nanotechnol.* **2008**, *3*, 682.
- (37) Chai, J. A.; Ĥuo, F. W.; Zheng, Z. J.; Giam, L. R.; Shim, W.; Mirkin, C. A. Scanning probe block copolymer lithography. *Proc. Natl. Acad. Sci. U. S. A.* **2010**, *107*, 20202.
- (38) Liu, G. L.; Eichelsdoerfer, D. J.; Rasin, B.; Zhou, Y.; Brown, K. A.; Liao, X.; Mirkin, C. A. Delineating the pathways for the site-directed synthesis of individual nanoparticles on surfaces. *Proc. Natl. Acad. Sci. U. S. A.* **2013**, *110*, 887.
- (39) Chai, J.; Liao, X.; Giam, L. R.; Mirkin, C. A. Nanoreactors for Studying Single Nanoparticle Coarsening. *J. Am. Chem. Soc.* **2012**, 134, 158.
- (40) Chen, P. C.; Du, J. S. S.; Meckes, B.; Huang, L. L.; Xie, Z.; Hedrick, J. L.; Dravid, V. P.; Mirkin, C. A. Structural Evolution of Three-Component Nanoparticles in Polymer Nanoreactors. *J. Am. Chem. Soc.* **2017**, 139, 9876.
- (41) Chen, P. C.; Liu, X. L.; Hedrick, J. L.; Xie, Z.; Wang, S. Z.; Lin, Q. Y.; Hersam, M. C.; Dravid, V. P.; Mirkin, C. A. Polyelemental nanoparticle libraries. *Science* **2016**, *352*, 1565.
- (42) Chen, P. C.; Liu, M. H.; Du, J. S. S.; Meckes, B.; Wang, S. Z.; Lin, H. X.; Dravid, V. P.; Wolverton, C.; Mirkin, C. A. Interface and heterostructure design in polyelemental nanoparticles. *Science* **2019**, *363*, 959.
- (43) Du, J. S.; Chen, P. C.; Meckes, B.; Xie, Z.; Zhu, J. H.; Liu, Y.; Dravid, V. P.; Mirkin, C. A. The Structural Fate of Individual Multicomponent Metal-Oxide Nanoparticles in Polymer Nanoreactors. *Angew. Chem., Int. Ed.* **2017**, *56*, 7625.
- (44) Chen, P. C.; Liu, G. L.; Zhou, Y.; Brown, K. A.; Chernyak, N.; Hedrick, J. L.; He, S.; Xie, Z.; Lin, Q. Y.; Dravid, V. P.; O'Neill-Slawecki, S. A.; Mirkin, C. A. Tip-Directed Synthesis of Multimetallic Nanoparticles. *J. Am. Chem. Soc.* **2015**, *137*, 9167.
- (4S) Zhang, H. Y.; Kinnear, C.; Mulvaney, P. Fabrication of Single-Nanocrystal Arrays. *Adv. Mater.* **2019**, 1904551.
- (46) Flauraud, V.; Mastrangeli, M.; Bernasconi, G. D.; Butet, J.; Alexander, D. T. L.; Shahrabi, E.; Martin, O. J. F.; Brugger, J. Nanoscale topographical control of capillary assembly of nanoparticles. *Nat. Nanotechnol.* **2017**, *12*, 73.
- (47) Giovannetti, R. The Use of Spectrophotometry UV-Vis for the Study of Porphyrins. In *Macro to Nano Spectroscopy*; Uddin, J., Ed.; IntechOpen, 2012; p 87.